Bioorganic & Medicinal Chemistry 17 (2009) 2544–2554

Contents lists available at ScienceDirect

Bioorganic & Medicinal Chemistry

journal homepage: www.elsevier.com/locate/bmc

Effect of 3,4-ethylenedioxy-extension of thiophene core on the DNA/RNA binding properties and biological activity of bisbenzimidazole amidines

Ivana Stolić [a], Katarina Mišković [b], Anahi Magdaleno [c], Ariel Mariano Silber [c], Ivo Piantanida [d], Miroslav Bajić [a,*], Ljubica Glavaš-Obrovac [b,*]

[a] Department of Chemistry and Biochemistry, Faculty of Veterinary Medicine, University of Zagreb, Heinzelova 55, 10000 Zagreb, Croatia
[b] Department of Medical Chemistry and Biochemistry, School of Medicine, J.J. Strossmayer University of Osijek, 31000 Osijek, Croatia
[c] Department of Parasitology, Institute of Biomedical Sciences, University of São Paulo, São Paulo, Brazil
[d] Division of Organic Chemistry and Biochemistry, Ruđer Bošković Institute, Zagreb, Croatia

ARTICLE INFO

Article history:
Received 2 October 2008
Revised 20 January 2009
Accepted 22 January 2009
Available online 5 February 2009

Keywords:
Benzimidazole amidine
DNA/RNA binding
Antiproliferative activity
Antiparasitic activity

ABSTRACT

Novel bisbenzimidazoles (**4**–**6**), characterized by 3,4-ethylenedioxy-extension of thiophene core, revealed pronounced affinity and strong thermal stabilization effect toward ds-DNA. They interact within ds-DNA grooves as dimmers or even oligomers and agglomerate along ds-RNA. Compounds **4**–**6** have shown moderate to strong antiproliferative effect toward panel of eight carcinoma cell lines. Compound **5** displayed the best inhibitory potential and in equitoxic concentration ($IC_{50} = 1 \times 10^{-6}$ M) induced accumulation of cells in G2/M phase after 48 h of incubation. Fluorescence microscopy showed that **5** entered into live HeLa cells within 30 min, but did not accumulate in nuclei even after 2.5 h. Compound **5** inhibited the growth of *Trypanosome cruzi* epimastigotes ($IC_{50} = 4.3 \times 10^{-6}$ M).

1. Introduction

In recent years many efforts have been focused at targeting specific sequences of macromolecules, especially specific DNA sequences, with the aim at designing both leads for medicinal chemistry and molecular probes for DNA polymorphism.[1–3] Natural products and synthetic organic cations that bind specifically and selectively to the DNA minor groove have therapeutic potential in a wide range of applications. These compounds bind to minor groove by a combination of ionic, hydrophobic and hydrogen bonding interaction.[4–6] For this purpose small molecules have to meet 'classical' structural criteria for optimum DNA fit and interaction: a crescent shape that complements the helical DNA minor groove, recognition units (H-bond donors and acceptors) on the side of the molecule facing DNA, cationic centre at terminals of the molecules to enhance electrostatic interactions, and an extended unfused heterocyclic structure to allow optimization of the compound for DNA minor groove interactions.[7–9]

Aromatic diamidines which have been shown to fit snugly into the minor groove of DNA and interact selectively with AT-rich sequences exhibited outstanding antimicrobial activity as well as antitumor bioactivity cells resistant to cisplatinum.[10–18] Although the mechanism of action of aromatic diamidines is not fully elucidated, it has been proven that their bioactivity is the result of DNA binding and subsequent inhibition of DNA-dependent enzymes (topoisomerases, polymerases, and nucleases) or possibly by direct inhibition of transcription.[10,19] A large number of DNA minor groove binders containing one or more benzimidazole heterocycles have been reported to date reveal promising antitumor and antiparasitic activities.[5,10,20–23] Benzimidazole units are often key structural elements in the aromatic frame work for the more effective diamidines.[24,25] In addition, an important role in determining biological activity and DNA binding affinity also plays the structure and the rigidity of the linker between the two aromatic amidine moieties.[16,25] Biophysical studies of previously synthesized minor groove binding compounds have suggested that structural features that increase van der Waals interactions of small molecules with the walls of the groove should increase the DNA affinity of these molecules.[7,26,27] On the basis of our previous research on aromatic diamidine in benzo[*c*]thiophene series,[28] three new bisbenzimidazole amidines (**4**–**6**) with 3,4-ethylenedioxythiophene as central unit were synthesized and their biological potential and binding affinity using calf thymus DNA, and ds-RNA (poly A-poly U) were studied. The crescent shape of the new compounds matches the curvature of the minor groove of DNA. The 3,4-ethylenedioxy extension of thiophene core in the central unit should increase electron-donating

* Corresponding authors. Fax: +385 1 2441390 (M.B.), +385 31 512 227 (L.G.-O.).
E-mail addresses: mbajic@vef.hr (M. Bajić), glavas-obrovac.ljubica@kbo.hr (L. Glavaš-Obrovac).

0968-0896/$ - see front matter © 2009 Elsevier Ltd. All rights reserved.
doi:10.1016/j.bmc.2009.01.071

capabilities and possibility for hydrogen bonding and/or van der Waals interactions and we expected this structural change to increase affinity and selectivity of these molecules for specific DNA sequences. We also report here on the cytotoxic effects of novel heterocyclic diamidines on a panel of eight carcinoma cell lines as well as their antiparasitic activity again *Trypanosome cruzi*, a protozoan parasite which affect 12–15 million people (http://www.who.int/ctc/chagas/disease.htm), and for which little therapeutic options are available.[29]

2. Results

2.1. Chemistry

The synthesis of bisbenzimidazolamidines **4–6** is outlined in Scheme 1 and is patterned after the approach developed to make the corresponding furan analogues.[20] The 3,4-ethylenedioxythiophene-2,5-dicarboxaldehyde (**3**),[30] a key precursor for bisbenzimidazoles was prepared in two steps from diethyl 3,4-ethylenedioxythiophene-2,5-dicarboxylate (**1**).[31] Diester **1** was first reduced by $LiAlH_4$ in THF to the corresponding diol **2**.[32] Diol was than oxidized with 1-hydroxy-1,2-benziodoxol-3(1*H*)-one 1-oxide (IBX)[33] previously prepared from 2-iodobenzoic acid, to obtain dialdehyde **3**. The key step in further reactions was formation of benzimidazole rings. In each case an aldehyde **3** was allowed to react with a substituted 1,2-phenylenediamine in the presence of 1,4-benzoquinone as the aromatizing agent.[20] In the cases of preparation of **4–6**, the amidino unit was preformed and was the substituent on the phenylenediamine ring.

2.2. Spectroscopy

The UV–vis spectra of all studied compounds were linearly dependent on concentration in the range $c(\mathbf{4}–\mathbf{6}) = 1 \times 10^{-6}$–$5 \times 10^{-5}$ mol dm^{-3} and the UV/vis spectra of **4–6** revealed negligible temperature dependent changes (25–90 °C) and excellent reproducibility upon cooling to 25 °C. Aforementioned results do not support intermolecular interactions between two or more molecules of studied compounds at experimental conditions used.

Furthermore, the UV–vis spectra of **4–6** in buffered aqueous solutions and corresponding molar extinction coefficients (ε) are quite similar (Table 1).

It is well known that amidine groups are protonated in weakly basic aqueous medium. By measuring the changes in the UV–vis spectra of studied compounds as a function of pH we have calculated pK values (pK(**4**) = 10.6 ± 0.2, pK(**5**) = 10.84 ± 0.03, pK(**6**) = 10.84 ± 0.05), the values are quite characteristic for amidines.[34] Comparison of the obtained pK values revealed negligible impact of the substituent attached to the amidine group.

2.3. Interactions of 4–6 with double stranded (ds-) DNA and RNA

2.3.1. UV–vis and CD titrations

Addition of any ds-polynucleotide resulted in pronounced batochromic and hypochromic effects of UV–vis spectra of **4–6** (data not shown). However, clear deviations from isosbestic points as well as shifts of absorption maxima in opposite directions depending on a compound/polynucleotide ratio strongly supported simul-

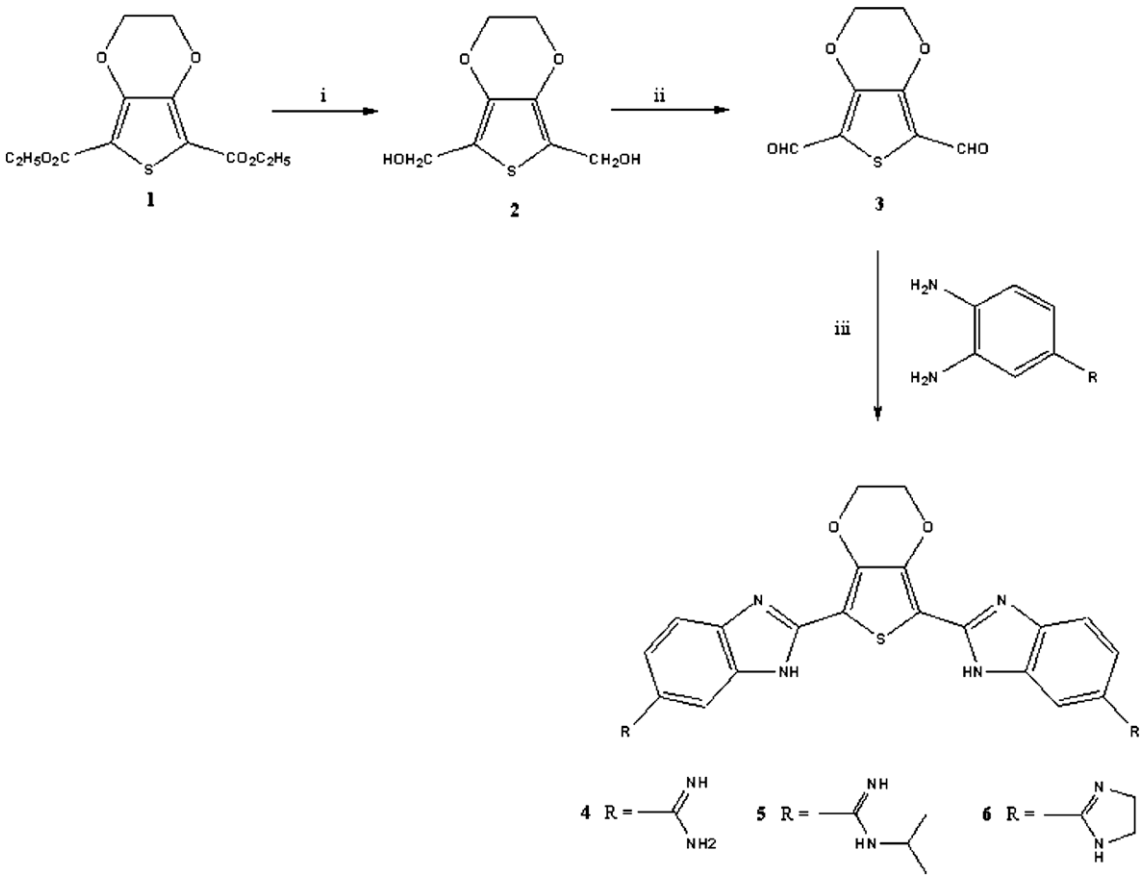

Scheme 1. Reagents and conditions: (i) $LiAlH_4$/THF; (ii) IBX, DMSO; (iii) 1,4-benzoquinone, EtOH.

Table 1
Electronic absorption data of **4–6**[a]

	λ_{max}/nm	$\varepsilon \times 10^3$/dm^3 mol^{-1} cm^{-1}
4	372	39.29
5	382	52.05
6	376	41.76

[a] Sodium cacodylate buffer, $I = 0.05$ mol dm^{-3}, pH 7.

taneous formation of more different complexes. At higher excess of polynucleotide over compound precipitation was observed. Due to all aforementioned reasons, it was not possible to process the UV–vis titration data by means of Scatchard equation[35] in order to determine affinity of compounds toward DNA/RNA.

To get insight into the changes of polynucleotide properties induced by small molecule binding, we have chosen CD spectroscopy as a highly sensitive method toward conformational changes in the secondary structure of polynucleotides.[36] In addition, achiral small molecules like **4–6** can eventually acquire induced CD spectrum (ICD) upon binding to polynucleotides, from which mutual orientation of small molecule and polynucleotide chiral axis could be derived, consequently giving useful information about modes of interaction.[37]

The addition of **4–6** to the *calf thymus* (ct-) DNA resulted in dramatic changes of the CD spectrum of ct-DNA (Fig. 1). Deviations from the isoelliptic points and changes of the CD bands of DNA in the opposite directions depending on the ratio $r_{[\mathbf{4-6}]/[\text{ct-DNA}]}$, strongly support simultaneous formation of more different complexes.

For all compounds at conditions of higher ct-DNA excess over compound ($r_{[\mathbf{4-6}]/[\text{ct-DNA}]} = 0–0.2$) strong induced CD (ICD) exciton signal appeared around absorption maxima of compounds above 300 nm, characterised by negative band at about $\lambda = 310–320$ nm and positive band between $\lambda = 350–450$ nm (Fig. 1). Since compounds **4–6** do not have any intrinsic CD spectrum, such a strong bisignate exciton ICD signal most likely resulted from the binding of **4–6** molecule dimers into the minor groove of ct-DNA.[36,38]

However, changes of the ICD exciton signals of studied compounds ($\lambda > 300$ nm) at higher ratios $r_{[\mathbf{4-6}]/[\text{ct-DNA}]} > 0.3$, differed considerably between compounds. Namely, increase of the ratio $r_{[\mathbf{4}]/[\text{ct-DNA}]}$ resulted in dramatic changes of exciton ICD signal of **4**, whereby strongly positive band at $\lambda = 350–450$ nm gradually diminished and for ratios $r_{[\mathbf{4}]/[\text{ct-DNA}]} > 0.3$ switched to strongly negative band. Unlikely to that, exciton ICD signal of **5** upon increase of the ratio $r_{[\mathbf{5}]/[\text{ct-DNA}]}$ changed only the shape of positive band at $\lambda = 320–450$ nm but not the sign. In contrast to **4** and **5**, exciton ICD signal of **6** retained its shape, while the relative intensity of positive band at $\lambda = 320–450$ nm increased proportionally with the increase of ratio $r_{[\mathbf{6}]/[\text{ct-DNA}]}$. The origins of such dramatic differences are most likely the steric and/or electronic properties of the substituents attached to the amidines of **4–6**.

The molecule with unsubstituted amidines (**4**) is significantly less sterically hindered and therefore can form within ds-DNA grooves more different dimers and oligomers, and the equilibrium among these forms is strongly dependent on the ratio $r_{[\mathbf{4}]/[\text{ct-DNA}]}$. The most probable explanation would be that similarly as found for pseudoisocyanine dye (PIC),[38] at higher excess of DNA over **4** ICD exciton signal of dimer should prevail, while oligomers formed at higher ratios ***r*** would have different ICD exciton signal.

The attachment of isopropyl-substituents to amidines somewhat restricted dimerisation and oligomerisation possibilities of **5** within DNA grooves, thus yielding less pronounced changes of ICD exciton signals. Finally, bulky imidazolyl-substituted amidines of **6** allowed only one type of oligomerisation within DNA grooves

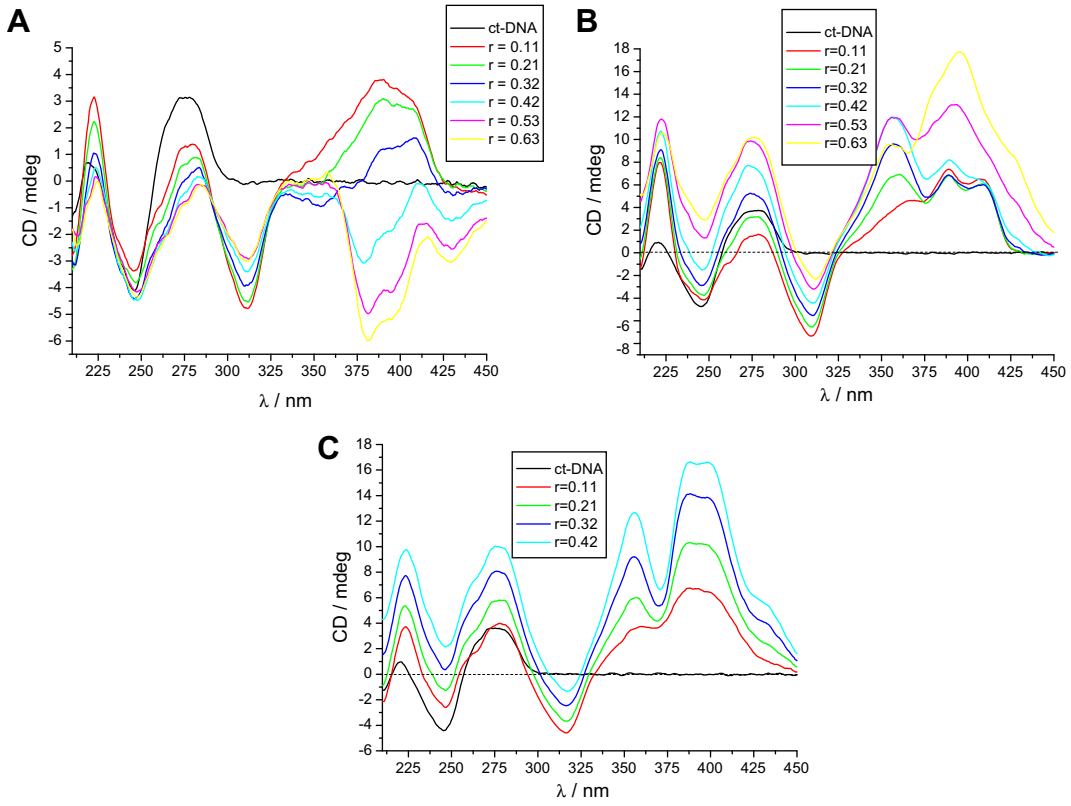

Figure 1. CD titrations of ct-DNA ($c = 4.6 \times 10^{-5}$ mol dm^{-3}) with **4** (A), **5** (B) and **6** (C), ratios $r_{[\mathbf{4,5}]/[\text{ct-DNA}]} = 0, 0.11, 0.21, 0.32, 0.42, 0.53, 0.63$; $r_{[\mathbf{6}]/[\text{ct-DNA}]} = 0, 0.11, 0.21, 0.32, 0.42$; at pH 7 (sodium cacodylate buffer, $I = 0.05$ mol dm^{-3}).

(most likely dimer formation within the DNA minor groove), in that way giving uniform ICD exciton signal, whose intensity was proportional to ratio $r_{[\mathbf{6}]/[\text{ct-DNA}]}$.

Addition of **4**–**6** to the ds-RNA (poly A–poly U) yielded somewhat different changes in the corresponding CD spectra (Fig. 2), if compared to the ds-DNA experiments (Fig. 1). For all compounds moderate (**4**) to strong (**5**, **6**) induced CD (ICD) bisignate exciton signal appeared, characterised by negative band at about λ = 350–360 nm and positive band between λ = 370–400 nm. Since compounds **4**–**6** do not have any intrinsic CD spectrum, such bisignate exciton ICD signal most likely resulted from the formation of **4**–**6** molecule agglomerates along the ds-RNA.[38]

2.3.2. Thermal denaturation experiments

Addition of studied compounds **4–6** resulted in strong stabilization of ds-DNA against thermal denaturation, while did not yield any significant effect on thermal denaturation of ds-RNA (Table 2). Furthermore, the nonlinear dependence of ΔT_m values on the ratio ***r*** suggested saturation of binding sites at ***r*** = 0.05–0.1. According to the CD experiments done at corresponding ratios ***r***, most likely dimmers of **4**–**6** positioned within the DNA minor groove are responsible stabilization of double stranded helix.

Lack of any significant ds-RNA stabilization by **4–6** suggested that ICD exciton signals in the CD experiments are related to the interaction between molecules of **4**–**6** and so formed aggregates do not stabilize significantly with ds-RNA. Namely, aromatic parts of **4**–**6** would tend to stack together in aqueous medium if not prevented by repulsion of positively charged amidines. However, an interaction with negatively charged RNA backbone neutralizes such repulsions and therefore along the ds-RNA corresponding agglomerates could be formed.

Table 2
The [a]ΔT_m values (°C) of studied polynucleotides upon addition of different ratios [b]***r*** of **4**, **5**, **6** at pH 7.0 (buffer sodium cacodylate, I = 0.05 mol dm^{-3})

[b]***r***=	ct-DNA				Poly A–poly U		
	0.05	0.1	0.2	0.3	0.1	0.2	0.3
4	12.7	14.4	13.9	12.9	—	−0.3	−0.9
5	11.7	>15.4[c]	>15.4[c]	—	0.9	0.8	—
6	12.2	11.9	11.4	12.3	0.4	0.3	−0.2

[a] Error in ΔT_m: ±0.5 °C.
[b] ***r*** = [compound]/[polynucleotide].
[c] ΔT_m not possible to calculate since T_m is over 100 °C.

2.3.3. Ethidium bromide displacement experiments

Due to the mixed binding modes of studied compounds toward ds-DNA, it was not possible to calculate binding constants and Scatchard ratios n.[39] As an alternative method for estimation of affinity, at least as a comparison of ability of studied molecules to compete for binding with classical intercalator already bound to DNA,[40] we have performed ethidium bromide (**EB**) displacement assay (Fig. 3).

The obtained IC_{50} values (Fig. 3) suggest that studied compounds show high cumulative affinity toward ct-DNA comparable to the affinity of **EB** (Ks = 10^6 M^{-1}).[41]

To summarize, the observed difference between ds-DNA and ds-RNA thermal stabilization induced by **4–6** is most likely the consequence of significantly different secondary structures of polynucleotides,[42] because of which DNA minor groove targeting compounds exhibit highly selective or even specific interactions with DNA in respect to RNA.[1] Moreover, distinct differences in the ICD bands of **4–6** upon mixing with ds-DNA and ds-RNA also agree with differences

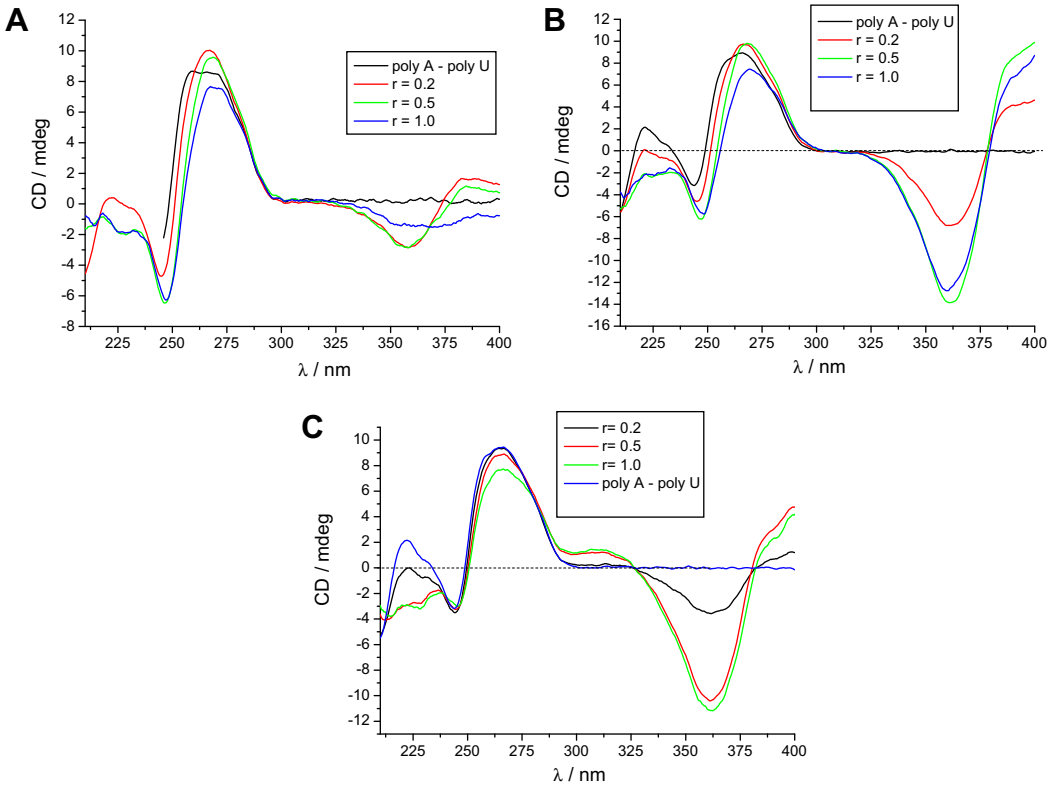

Figure 2. CD titrations of poly A–poly U (c = 3.0 × 10^{-5} mol dm^{-3}) with **4** (A), **5** (B) and **6** (C), ratios $r_{[\mathbf{4-6}]/[\text{poly A–poly U}]}$ = 0, 0.2, 0.5, 1 at pH 7 (sodium cacodylate buffer, I = 0.05 mol dm^{-3}).

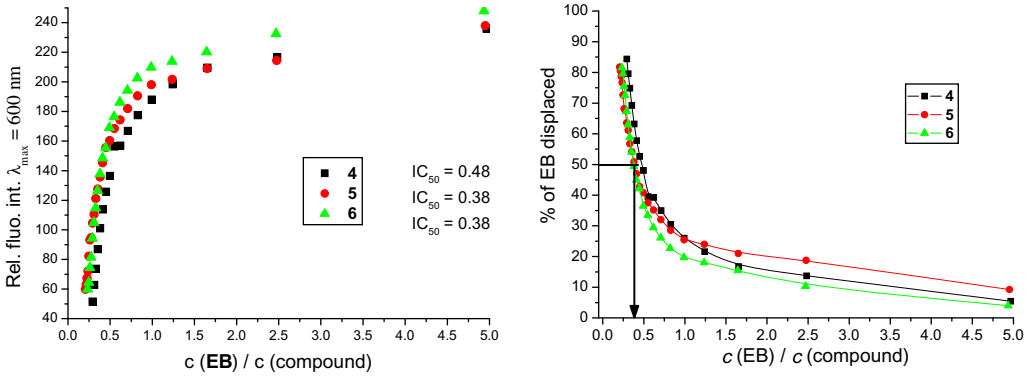

Figure 3. Ethidium bromide (**EB**) displacement assay: to ct-DNA solution ($c = 5 \times 10^{-5}$ mol dm^{-3}) ethidium bromide ($c = 5 \times 10^{-6}$ mol dm^{-3}) was added (***r*** ([**EB**]/[ct-DNA] = 0.1), and quenching of the **EB**/DNA complex fluorescence emission (λ_{ex} = 520 nm, λ_{em} = 601 nm) was monitored as function of c(**EB**)/c(compound). The given IC_{50} values present the ratio c(**EB**)/c(compound) = [Int(**EB**/DNA) − Int($\mathbf{EB}_{free}$)]/2, where Int(**EB**/DNA) is fluorescence intensity of **EB**/DNA complex and Int($\mathbf{EB}_{free}$) is fluorescence intensity of the free ethidium bromide before DNA is added.

in secondary structures of polynucleotide double helices. Finally, strong thermal stabilization effect of **4–6** agrees well with IC_{50} values of ethidium bromide displacement experiments, pointing toward strong binding of studied compounds to ds-DNA.

2.4. Biological results

2.4.1. Antitumor effects

Since there is a constant need for new more effective and less harmful potential anticancer drugs we studied antiproliferative capacity of three novel benzimidazoyl hydrochloride analogues on different solid tumor cell lines, derived from carcinoma of different origin (MCF-7, AGS, NCI-H358, HEp2, Caco-2, HeLa, HT-29, and MiaPaCa). The mentioned cell lines were chosen according to their sensitivity on the chemotherapeutic action. Most of them are resistant or semiresistant to chemotherapeutics used in standard clinical settings.

Obtained data show that investigated compounds differentially influenced tumor cells' growth, depending on the cell line as well as on the dose applied (Fig. 4). Compound **5** displayed the best antiproliferative capacity against all treated cell lines compared to control non-treated cells (Fig. 4B). The human breast adenocarcinoma cell line (MCF-7) was most sensitive on the antiproliferative effects of investigated compounds. Novel compounds **4–6** and Hoechst 33258, statistically significantly inhibited the growth of MCF-7 cells in all concentration applied (10^{-7}–10^{-4} M). Compound **5** was the most efficient and applied in concentration 10^{-7} M inhibited growth of MCF-7 for more than 40% in comparison with control non-treated cells (Fig. 4B). Compound **5** at a relatively low concentration of 10^{-6} M displayed also the best inhibitory effect against human cervix adenocarcinoma (HeLa) and human larynx carcinoma (HEp-2) cells compared to compounds **4** and **6,** as well as Hoechst 33258, which were markedly less effective on these cell lines. It caused inhibition in HeLa and

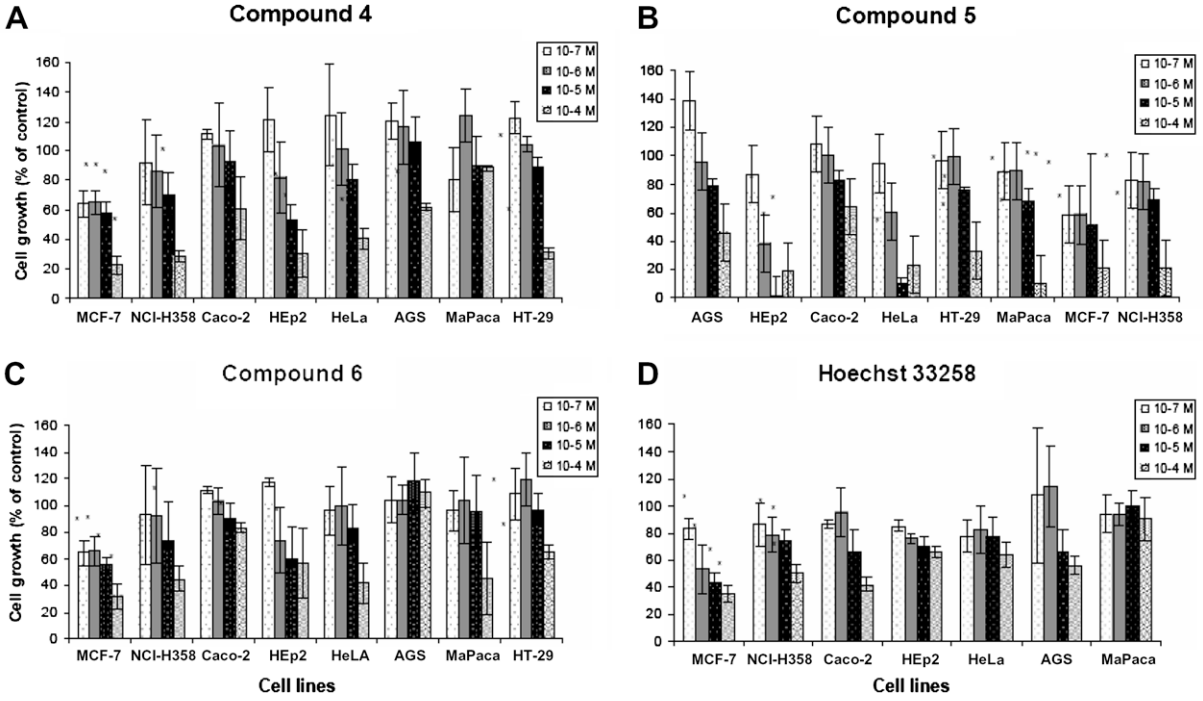

Figure 4. Effects of investigated compounds **4–6** and Hoechst 33258 on solid tumors cells growth following 72 h incubation (10^{-4}–10^{-7} M). Data are shown as a mean values from three independent experiments done in threeplicate ± SD. Statistically significant change ($p < 0.05$) is presented by *.

HEp-2 cells proliferation by more than 40% and 80%, respectively. Applied in a concentration of 10^{-5} M compounds **4** and **6** statistically significant slowed down the growth of MCF-7, NCI-H358, HEp-2, and HT-29 cells. Investigated compounds **4** and **6** had no significant effect on the growth of Caco-2, MIAPaCa2 and AGS cells.

2.4.2. Cell cycle perturbations

To reveal the inhibitory mechanism of compound **5** on cell proliferation, cell cycle analysis is performed by staining nuclear DNA with propidium iodide, and cells classified into G_1, S and G_2/M phases according to fluorescent intensity. HeLa cells were exposed to equitoxic ($IC_{50} = 1 \times 10^{-6}$ M) concentration of compound **5** in order to discover the potential of compound **5** to induce cell cycle perturbations in different time of exposure. Changes in the cell cycle of the cells exposed to compound **5** and Hoechst 33258 (1×10^{-5} M) in comparison with control cells after the first 24 h of incubation were not observed. Cells passed G1 restriction checkpoint and entered into S phase in the first 24 h of incubation (data not shown).

As shown in Table 3, 48 h after addition of compound **5** the percentage of cells in G_0/G_1 phase started decreasing compared with control cells, and the percentage of cells in S phase began increasing, meaning that the G_0/G_1 to S progression was conducted in response to stimulation by compound **5**. In treated cells, 72 h after addition of compound **5**, the percentage of cells in S phase started decreasing, and the percentage of cells in G_2/M phase began increased meaning that the S to G_2/M progression was subsequently executed. A significant drug induced accumulation of cells in the G_2/M phase was perceived (Table 3) in by compound **5** treated cells. The G_2/M block started 24 h after treatment and a continuous increase in the number of cells accumulated in these phase was noticeable until 48 h. A slightly increase of number G_2/M phase cells, compared by number of cells after 48 h of incubation, was observed after 72 h of incubation. In addition, in the Hoechst 33258 treated cells, the changes in cell cycle of treated cells in comparison with control cells were not observed after 24 and 48 h of incubation. Drug-induced accumulation of cells in the G_2/M compartment was visible as late as after 72 h of incubation.

2.4.3. Intracellular distribution

The compound **5** in the concentration of 1×10^{-5} M passed HeLa cell's membrane and entered into HeLa cell's cytoplasm within 30 min. After administration (60 min), compound **5** was located mainly near the cell membrane and uniformly distributed in the cytoplasm (Fig. 5A). Within the limits of fluorescence detection, there is no evidence of nuclear uptake 2.5 h after tested compound administration. At the same experimental condition, a minor groove binder—Hoechst 33258 came to the nucleus of HeLa cells after 30 min of incubation.

2.4.4. The effect of investigated compounds on the growth of *T. cruzi* epimastigotes

The ability of investigated compounds to inhibit the *T. cruzi* epimastigote growth was evaluated by using two concentrations (1×10^{-5} and 1×10^{-4} M) which were considered not toxic to mammalian cell. The cell density in the LIT medium with compound **5** was significantly lower than of control ($p < 0.05$). However, no differences were observed when using compound **4** or compound **6** (Fig. 6). As **5** was the only compound showing an effect on epimastigote growth, additional concentrations (between 1×10^{-6} M and 1×10^{-5} M) were evaluated in order to obtain the IC_{50}, being this value $4.25 \pm 0.08 \times 10^{-6}$ M (day five). To obtained the IC_{50}, 1, 2.5, 5, 7.5 and 10 μM compound **5**, were evaluated. The IC_{50} was $2.4 \pm 0.2 \times 10^{-6}$ M.

Table 3
Cell cycle perturbation induced by compound **5** and Hoechst 33258

Treatment	Cell percentage (% ± standard deviation)					
	G0/G1		S		G2/M	
	48 h	72 h	48 h	72 h	48 h	72 h
Control	56.7 ± 1.9	61.8 ± 0.9	29.0 ± 5.2	20.1 ± 0.1	14.3 ± 3.3	18.2 ± 0.9
Compound **5** (10^{-6} M)	46.9 ± 0.4	33.6 ± 6.5	30.7 ± 3.5	43.1 ± 6.0	22.4 ± 3.8	23.4 ± 0.5
Hoechst (10^{-5} M)	49.8 ± 0.9	46.3 ± 2.2	35.0 ± 5.7	23.9 ± 1.2	15.2 ± 6.6	29.9 ± 0.8

Data represent percentages of HeLa cells in different phases of cell cycle (G0/G1; S and G_2/M) after treatment with compound **5** (10^{-6} M) and Hoechst 33258 (10^{-5} M) for 48 and 72 h. Cell cycle analysis was performed by flow cytometry as described in 'Materials and Methods;. Data represent the mean ($n = 3$).

Figure 5. Fluorescence microscopy analysis of entry and intracellular distribution of 10^{-5} M compound **5** (A) and Hoechst 33258 (B) in HeLa cells after 60 min of incubation using filters BP 450-490, LP 520. Magnification: 400×.

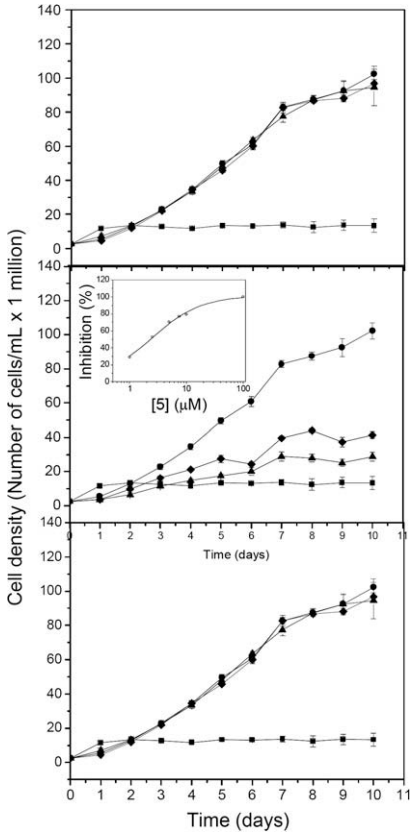

Figure 6. Epimastigotes cell growth in the presence of compound **4** (A), **5** (B) (inset: estimation of IC_{50} by the sigmoidal equation), and **6** (C). The cells were mock treated with water as control (●), supplemented with antimycin (0.5×10^{-6} M) and rotenone (2×10^{-4} M) (■); or treated with compounds at concentrations of 0.01 M (▲) or 0.1 M (♦).

2.4.5. The entry and distribution of compounds 4, 5 and 6 into *T. cruzi* epimastigotes

The entry and distribution of compounds **4**, **5** and **6** in *T. cruzi* was evaluated by fluorescence microscopy. Epimastigote cultures were incubated with 1×10^{-5} and 1×10^{-4} M of each compound for 30 min, 2 h, or overnight. The uptake of compounds **4**–**6** was not detected for up to 2 h of incubation. The fluorescent signal of compound **5** was in granulose structures resembling reservosomes (Fig. 7) after the overnight incubation.

3. Discussion

All studied compounds **4**–**6** exhibited pronounced cumulative affinity, as well as strong thermal stabilization effects toward ds-DNA. More detailed CD studies revealed that in contrast to the most of closely related benzimidazole-based diamidines studied by Wilson and co-workers,[43–46] **4**–**6** most likely do not interact within ds-DNA grooves as single molecules but presumably as dimers and/or even oligomers. Possible reason for that could be 3,4-ethylenedioxy- extension of thiophene core, which should significantly increase hydrophobicity in respect to previously studied thiophene and furan analogues.[8,43] Studied compounds also agglomerate along ds-RNA but these agglomerates do not stabilize significantly the polynucleotide double helix.

Since new synthesized bisbenzimidazolamidines **4**–**6** have a structure similar to well studied aromatic diamidines which show marked antimicrobial and antitumor bioactivity[14] and all of them showed marked ds-DNA activity, we investigated their antitumor potential on a panel of human carcinoma cells. As anticipated, obtained data show that novel compounds differentially influenced tumor cells' growth depending on the cell line as well as on the dose applied, but we cannot exclude that the differences in cytotoxicity are due to different cellular uptake.

Rapid cellular uptake and nuclear accumulation of benzimidazole-based amidines in different cancer cells has been recently evidenced by fluorescence microscopy.[47] In contrast, results of our study of uptake and intracellular distribution of the compound **5** show its very slow penetration through the membrane of HeLa cells. After administration (60 min), compound **5** was located mainly near the cell membrane and uniformly distributed in cytoplasm. Neither after 150 min of incubation was noticed its entry into nucleus. At the same experimental condition, a minor groove binder—Hoechst 33258 was localized in the nucleus of HeLa cells after 30 min of incubation. It is well known that chemical structure of compounds is a key determinant of their uptake and allocation in the live cells.[14,48] A mechanism by which compound **5** enters into cells is unknown at present but it seems that due to the increased hydrophobicity in respect to previously studied thiophene and furan analogues,[10,11] it is preferably accumulated within the cell membrane (Fig. 5).

Cell cycle analysis and detection of apoptosis are very important functional parameters to assess the cellular metabolism, physiology and pathology.[47,49] Cell division inhibition is a universal response to DNA damage. In eukaryotic cells, DNA-damaging agents cause the arrest of cells in the G_1 and G_2/M phase of the cell cycle. Presumably the delay in cell division enables the cells to repair damaged DNA and/or complete DNA replication.[50,51] It is well known that aneuploidy and genetic instability are a hallmark of the most of solid tumors, and they are thought to enhance tumor progression.[52] In cancer cells, satisfaction of mitotic and postreplication checkpoint is frequently delayed or prevented by various defects, some of which have been causally implicated in tumorigenesis. At the same time, deliberate induction of postreplication and mitotic arrest has proved clinically useful, as antimitotic drugs that interfere with proper chromosome-spindle interactions are effective anticancer agents.[53] However, how mitotic arrest contributes to tumorigenesis or antimitotic drug toxicity is not well defined.

Since the compound **5** displayed the best antiproliferative capacity against all treated cell lines, in an attempt to explore the molecular mechanisms underlying the observed cytotoxic response, cell cycle analysis was conducted. The presented cell cycle experiment indicates that compound **5** treatment induces significant accumulation of HeLa cells in the G_2/M phase after 48 h of incubation. The G_2/M block started 24 h after treatment and a continuous increase in the number of cells accumulated in these phase was noticeable. In addition, in the minor groove binder Hoechst 33258 treated cells, the changes in cell cycle of treated cells in comparison with control cells were not observed after 24 and 48 h of incubation. Drug-induced accumulation of cells in the G_2/M compartment was visible as late as after 72 h of incubation.

Whether is observed antiproliferative effect of novel bisbenzimidazoles on the growth of tumor cells due to their DNA binding capacity, or their inhibitory effects on transcription and replication processes, or just as a part of multistep processes remains to be investigated.

Study of antiparasitic activity of novel compounds showed that only compound **5** is active, showing an inhibitory effect on the *T. cruzi* epimastigotes growth with an IC_{50} of 2.4 ± 0.2 μM. Observed IC_{50} value is significantly lower than IC_{50} antiproliferative effect obtained for mammalian cells. As displayed in Figure 7, compound **5** is the only among studied compounds that could be taken up by *T. cruzi*, what clearly explained its trypanocidal activity. Interestingly, compound **5** seems to accumulate in a trypanosomatid organelle called reservosome, which are endocytic organelles from *T.*

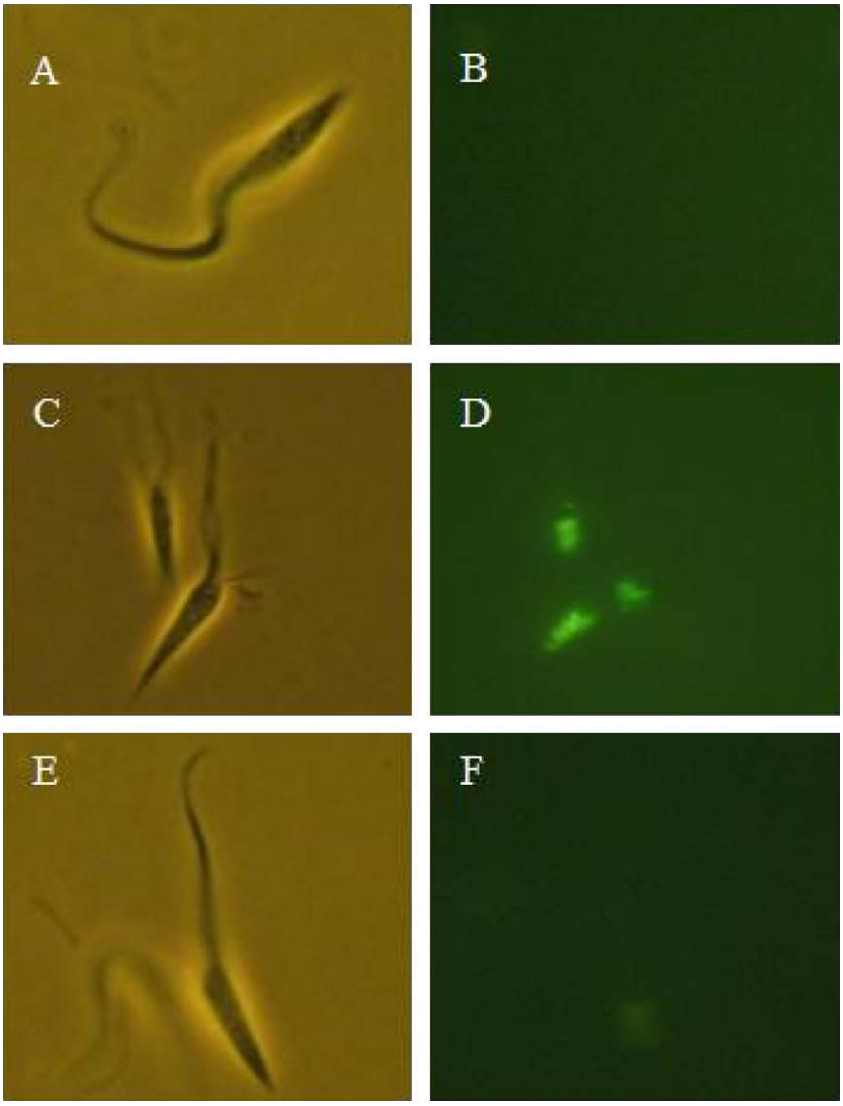

Figure 7. Epimastigotes of *T. cruzi* cultured overnight with the three compounds at 1×10^{-4} M. Figures A, C and E show the parasites cultured with compounds **4**, **5** and **6**, respectively in light field, and figures B, D and F show the same parasites at fluorescence microscopy. Magnification ×1000.

cruzi epimastigotes that store proteins and lipids as reserve substances for future uses.[54] Since we were not able to detect nuclei or kinetoplast staining, it remains unclear the way compound **5** is toxic for the cells. However, it could be the case that little quantities (below of our detection capacity) of DNA bound compound **5** could be toxic for these cells. Our results prompt compound **5** as an interesting compound in the search of new therapeutic drugs against parasitic diseases caused by trypanosomatid parasites, in particular the Chagas' illness. Further studies on infective stages of *T. cruzi* will be carried out.

4. Experimental

4.1. Synthesis

Solvents were distilled from appropriate drying agents shortly before use. TLC was carried out on DC-plastikfolien Kieselgel 60 F254, Merck. Melting points were determined on a Büchi 510 melting point apparatus and were uncorrected. IR spectra [ν_{max}/cm^{-1}] were obtained for KBr pellets on a Perkin–Elmer 882 spectrophotometer. The ^{1}H NMR spectra were recorded on a Bruker Avance 300 MHz spectrometer. The ^{13}C NMR spectra were recorded on a Bruker Avance 600 MHz spectrometer but due to the poor solubility only few signals were obtained for compound **5**, while spectra of compounds **4** and **6** could not be accurately interpreted. Chemical shifts (δ/ppm) are referred to TMS. Mass spectra were recorded on a Waters Micromass Q-ToF micro. Elemental analyses were performed by Microanalytical laboratory at the Ruđer Bošković Institute.

4.1.1. 3,4-Ethylenedioxythiophene-2,5-diol (2)

Diethyl 3,4-ethylenedioxythiophene-2,5-dicarboxylate (1.45 g, 5.07 mmol) dissolved in THF (70 mL) was added to a suspension of $LiAlH_4$ (0.92 g, 0.0243 mol) in dry THF (100 mL). The reaction mixture was stirred for 3 h at 0 °C, and then for 1 h at room temperature. When reaction was finished ethanol was added, and resulting suspension was filtered, filtrate evaporated and dried under vacuum yielding 0.983 g (87.9%) pale brown powder: mp 135–136 °C; IR (cm^{-1}) in KBr: 3364, 3299, 1520, 1449, 1345, 1122, 992, 651; ^{1}H NMR (δ, DMSO-d_6, 25 °C, ppm): 5.16 (t, 2H, J = 5.61 Hz, OH), 4.41 (d, 4H, J = 5.61 Hz, –CH_2OH), 4.16 (s, 4H, OCH_2CH_2O).

4.1.2. 3,4-Ethylenedioxythiophene-2,5-dicarboxaldehyde (3)

To a solution of 1-hydroxy-1,2-benziodoxol-3(1*H*)-one 1-oxide (IBX) (6.172 g, 0.022 mol) in DMSO (32 mL) compound **2** (1.272 g, 6.3 mmol) in DMSO (73 mL) was added. Reaction is monitored by

TLC, after 4 days at the room temperature, reaction mixture was poured into water. The resulting precipitate was collected by filtration and recrystallized from EtOH–H_2O yielding 0.824 g (66%) of pale brown powder: mp 140–141 °C (Lit.[30] 141 °C); IR (cm^{-1}) in KBr: 2927, 1667, 1503, 1463, 1267, 1103, 1082, 694; ^1H NMR (δ, $CDCl_3$, 25 °C, ppm): 10.04 (s, 2H, CHO), 4.46 (s, 4H, –OCH_2CH_2O–).

4.1.3. 2,5-Bis[2-(5-amidinobenzimidazoyl)]-3,4-ethylenedioxythiophene dihydrochloride (4)

A solution of 3,4-etylenedioxythiophene-2,5-dicarboxaldehide (0.058 g, 0.291 mmol), 4-amidino-1,2-phenylenediamine (0.087 g, 0.583 mmol), and 1,4-benzoquinone (0.064 g, 0.591 mmol) in ethanol (40 mL) was heated at reflux for 4 h (under nitrogen). The reaction mixture was cooled to room temperature, and the dark solid was collected by filtration and washed with anhydrous ether. The solid was dissolved in HCl-saturated ethanol and stirring overnight. Green solid was collected by filtration, washed with anhydrous ether, and dried under vacuum to yield 0.057 g (42.6%) of green powder, mp > 250 °C; IR (cm^{-1}) in KBr: 3193, 1672, 1626, 1601, 1512, 1488, 1453, 1088, 982, 816; ^1H NMR (δ, DMSO-d_6, 25 °C, ppm): 12.66 (br s, 1H, NH), 9.37 (s, 4H, NH), 9.13 (s, 4H, NH), 8.15 (s, 2H, ArH), 7.79 (d, 2H, J = 8.47 Hz, ArH), 7.68 (dd, 2H, J = 8.47 Hz, J = 1.64 Hz, ArH), 4.67 (s, 4H, OCH_2CH_2O); HRMS: calcd for $C_{22}H_{19}N_8O_2S$ (M^++1), 459.1352; Found, 459.1329. Anal. Calcd for $C_{22}H_{18}N_8O_2S{\cdot}2HCl{\cdot}5H_2O$ (M_r = 621.50): C, 42.52, H, 4.87, N, 18.03, Cl, 11.41. Found: C, 42.25, H, 4.44, N, 18.07, cl, 11.61.

4.1.4. 2,5-Bis[2-(5-(*N*-isopropylamidino)benzimidazoyl)]-3,4-ethylenedioxythiophene dihydrochloride (5)

A solution of 3,4-etylenedioxythiophene-2,5-dicarboxaldehide (0.150 g, 0,757 mmol), 4-(*N*-isopropylamidino)-1,2-phenylenediamine (0.290 g, 1,516 mmol), and 1,4-benzoquinone (0.170 g, 1,577 mmol) in ethanol (100 mL) was heated at reflux for 4 h (under nitrogen). The reaction mixture was cooled to room temperature, and the dark solid was collected by filtration and washed with anhydrous ether. The solid was dissolved in HCl–saturated ethanol. After stirring overnight, the green solid was collected by filtration, washed with anhydrous ether, and dried under vacuum to yield 0.208 g (50.7%) of green powder, mp > 250 °C. IR (cm^{-1}) in KBr: 3395, 3223, 1669, 1613, 1488, 1088, 720; ^1H NMR (δ, DMSO-d_6, 25 °C, ppm): 9.55 (s+s, 2H, NH), 9.40 (br s, 2H, NH), 9.00 (s, 2H, NH), 8.01 (s, 2H, ArH), 7.78 (d, 2H, J = 8.59 Hz, ArH), 7.56 (d, 2H, J = 8.74 Hz, ArH), 4.67 (s, 4H, OCH_2CH_2O), 4.08 (m, 2H, J = 6.56 Hz, CH), 1.31 (d, 12H, J = 6.56 Hz, CH_3); ^{13}C NMR (δ, D2O, 25 °C, ppm): 161.4, 145.6, 140.6, 121.5, 106.7, 65.1, 45.9, 20,5 (only 8 of expected 13 signals were accurately determined, while intensity of 5 signals was too low); HRMS: calcd for $C_{28}H_{31}N_8O_2S$ (M^++1), 543.2291. Found, 543.2266. Anal. Calcd for $C_{28}H_{30}N_8O_2S{\cdot}2.5HCl{\cdot}4H_2O$ (M_r = 705.88): C, 47.64; H, 5.78; N, 15.87; Cl, 12.56. Found: C, 47.84; H, 5.74; N, 16.34; Cl, 12.75.

4.1.5. 2,5-Bis[5-(2-imidazolino)benzimidazol-2-yl]-3,4-ethylenedioxythiophene dihydrochloride (6)

A solution of 3,4-etylenedioxythiophene-2,5-dicarboxaldehide (0.6223 g, 3.1429 mmol), 4-(imidazoylamidino)-1,2-phenylenediamine (1.1188 g, 6.2854 mmol), and 1,4-benzoquinone (0.6929 g, 6.4157 mmol) in ethanol (200 mL) was heated at reflux for 8 h (under nitrogen). The reaction mixture was cooled to room temperature, and the dark solid was collected by filtration and washed with anhydrous ether. The solid was dissolved in HCl–saturated ethanol and stir overnight. Green solid was collected by filtration, washed with anhydrous ether, and dried under vacuum to yield 0.767 g (47.9%) of green powder, mp > 250 °C; IR (cm^{-1}) in KBr: 3465, 3201, 1600, 1513, 1487, 1366, 1090, 700; ^1H NMR (δ, DMSO-d_6, 25 °C, ppm): 12.81 (br s, 2H, NH), 10.62 (s, 4H, NH), 8.32 (s, 2H, ArH), 7.82 (br s, 4H, ArH), 4.67 (s, 4H, OCH_2CH_2O), 4.03 (s, 8H, NCH_2CH_2N); HRMS: calcd for $C_{26}H_{23}N_8O_2S$ (M^++1), 511.1665; found, 511.1646. Anal. Calcd for $C_{26}H_{22}N_8O_2S{\cdot}2HCl{\cdot}4H_2O$ (M_r = 655.56): C, 47.63; H, 4.92; N, 17.09. Found: C, 47.72; H, 4.95; N, 17.57.

4.2. Spectroscopic experiments

The electronic absorption spectra were obtained on Varian Cary 100 Bio spectrometer, CD spectra on JASCO J815 spectrophotometer and fluorescence spectra on the Varian Eclipse fluorimeter, all in quartz cuvettes (1 cm). The spectroscopic studies were performed in aqueous buffer solution (pH 7, sodium cacodylate buffer, I = 0.05 mol dm^{-3}). Under the experimental conditions absorbance of **4, 5, 6** was proportional to their concentrations. Polynucleotides were purchased from Sigma (poly A–poly U) and Aldrich (*calf thymus* (*ct*)-DNA). Polynucleotides were dissolved sodium cacodylate buffer, I = 0.05 mol dm^{-3}, pH 7. Calf thymus (*ct*-)DNA was additionally sonicated and filtered through a 0.45 μm filter. Polynucleotide concentration was determined spectroscopically as the concentration of phosphates. Spectroscopic titrations were performed by adding portions of polynucleotide solution into the solution of the studied compound.

Thermal melting curves for ds-DNA, ds-RNA and their complexes with studied compounds were determined as previously described by following the absorption change at 260 nm as a function of temperature. Absorbance of the ligands was subtracted from every curve, and the absorbance scale was normalized. The T_m values are the midpoints of the transition curves, determined from the maximum of the first derivative and checked graphically by the tangent method. ΔT_m values were calculated subtracting T_m of the free nucleic acid from T_m of the complex. Every ΔT_m value here reported was the average of at least two measurements, the error in ΔT_m is ±0.5 °C.

4.3. Biological experiments

4.3.1. Cell culturing

The experiments were carried out on 8 human cell lines: bronchoalveolar carcinoma (NCI-H358), cervical adenocarcinoma (HeLa), laryngeal carcinoma cells (HEp-2), pancreatic carcinoma cells (MIAPaCa2), colon carcinoma cells (HT-29, CaCo2), stomach epithelial gastric adenocarcinoma (AGS) and human breast adenocarcinoma cells (MCF-7).

Cells were grown as a monolayer in tissue culture flasks (250 ml; BD Falcon, Germany) in Dulbecco's modified Eagle medium (DMEM) with 10% fetal bovine serum (FBS) supplemented with 2 mM glutamine, 100 U of penicillin and 0.1 mg streptomycin. Cells were cultured in a humidified (95% air, 5% CO_2) CO_2 incubator (Shell Lab, Sheldon Manufacturing, USA) at 37 °C. The trypan blue dye exclusion method was used to assess cell viability.

4.3.2. Cell growth inhibition assay

Cytotoxic effects on tumor cell growth were determined using the MTT assay.[55] In general, investigated compounds were dissolved in dimethylsulfoxide (DMSO) as a 1×10^{-2} M stock. All working dilutions (10^{-3}–10^{-6} M) were prepared immediately before each experiment in high pure water. The DMSO was also tested for eventual inhibitory activity by adjusting its concentration to be the same as in working concentrations. At day zero of the experiment, the cells (2×10^4 cells/ml) were plated onto 96-microwell plates (Greiner, Austria, EU) and allowed to attach overnight in a CO_2 incubator (Shell Lab, Sheldon Manufacturing, USA). Later (24 h), the medium was replaced with a fresh medium containing various well defined concentrations of investigated compounds. Controls were grown under the same conditions without the addition of the test substances. After 72 h of incubation med-

ium was removed and 40 μl of MTT (5 mg/ml of phosphate buffered saline) was added. DMSO (160 μl) was added to each well to dissolve in water insoluble MTT-formazane crystals. The plates were transferred to an Elisa plate reader (Stat fax 2100, Pharmacia Biotech, Uppsala Sweden). The absorbency was measured at 570 nm on a microplate reader. All experiments were performed at least 3 times, with 3 wells each.

The percentage of cell growth (PG) was calculated by the following equation:

$$PG = (A - A_{BLANCK}/A_{CONTROL} - A_{BLANCK}) \times 100$$

BLANCK = medium without cells containing cytostatic and MTT.

4.3.3. Uptake and intracellular distribution of compound 5 and Hoechst 33285

HeLa cells were grown on microscopic slides (1×10^5 cells/slide) at 37 °C for 24 h. Cells were incubated with compounds **5** (10^{-5} M) and Hoechst 33258 (10^{-5} M) at different intervals (for 30 min, 60 min, 90 min, 120, and 150 min) than washed with PBS, covered with a glass coverslip and analyzed. Control cells, in order to confirm the cells viability, were treated in PI solution (0.01 μM) for 5 min, washed with PBS and analyzed under the microscope (PBS as mounting medium). The entry and intracellular distribution of tested chemicals were analyzed under the fluorescence microscope (Axioskop 2 MOT, Carl Zeiss Jena GmbH, Jena, Germany) with Zeiss filter combinations: BP 450-490 and LP 520.

4.3.4. Cell cycle analysis

For cell cycle analysis, HeLa cells (5×10^5 cells per well) were seeded into 6-well plates. Later (24 h) tested compound **5** and Hoechst 33285 were added at a concentration of 1×10^{-6} M and 1×10^{-5} M, respectively. Cells were harvested at different intervals (24, 48 and 72 h) following drug treatment. Floating and adherent cells were collected separately, than combined, washed with phosphate buffer saline (PBS), fixed with 70% ethanol, and stored at −20 °C. Immediately before the analysis, the cells were washed with PBS and resuspended in 1 μg/ml of propidium iodide (PI) and 0.2 μg/μl of RNAse A. The stained cells were then analyzed with Becton Dickinson FACScalibur (Becton Dickenson) flow cytometer (20,000 counts were measured). The percentage of the cells in each cell cycle phase was determined using the ModFit LT™ software (Verity Software House) based on the DNA histograms. The tests were performed in triplicates and repeated at least twice.

4.3.5. *Trypanosoma cruzi* culture and the growth inhibition assay

Epimastigote forms of *Trypanosoma cruzi* strain clone 14 were maintained in LIT medium supplemented with 10% fetal calf serum (FCS) at 28 °C. Cultures were maintained in an exponential growth phase for 8 days by passages each 48 h. Inhibition assays were carried out in 96 well plates containing 200 μL of LIT medium supplemented with 10% FCS. Negative control was LIT medium with 10% FCS. Positive control was LIT medium with 10% FCS and two inhibitors of respiratory chain: rotenone (2×10^{-4} M) and antimycin (0.5×10^{-6} M). Compounds **4**, **5** and **6** (0.1 M) were resuspended in H_2O and added to the culture medium at 1×10^{-4} M or 1×10^{-5} M as indicated in each case. Cell number was estimated every day during 8 days by absorbance reading at 620 nm (turbidimetry) and cell number was obtained by using calibration curves. The assays (each treatment) were carried out in eight replicas ($n = 8$). The inhibition percentages (% I_c) were estimated by taking into account the reached growth of each treatment with respect to the control at day five (middle exponential phase). The IC_{50} was estimated by using concentrations of 1, 2.5, 5, 7.5 and 10 μM. Obtained data were adjusted to a sigmoidal model equation. All the assays were performed at least in triplicates, and presented results correspond to representative experiments.

4.3.6. Uptake and intracellular distribution of investigated compounds into *T. cruzi*

Exponential growth phase epimastigotes were incubated with 1×10^{-5} M compound **5** for 30 min, 60 min, and overnight. The cells were then washed with PBS, and resuspended in PBS as mounting medium. The viability was checked by microscopic observation of flagellar motility. The entry and intracellular distribution of tested chemicals were analyzed under the fluorescence microscope (Axiophot, Carl Zeiss Jena GmbH, Jena, Germany) with Zeiss filter combinations: BP 450-490, LP 520 as previously described for mammalian cells.

Acknowledgments

This research was supported by Grants of Croatian Ministry of Science, Education and Sport No: 053-0982914-2965, 219-0982914-2176, 219-0982914-2179, 098-0982914-2918, and Fundação de Amparo à Pesquisa do Estado de São Paulo (FAPESP) 03/13257-8 to AMS. AM is a fellow of the Fundação de Amparo à Pesquisa do Estado de São Paulo (FAPESP). The authors wish to thank Igor Bratoš, PLIVA Croatia Ltd., Research & Development, for providing high-resolution mass spectral analyses.

References and notes

1. Demeunynck, M., Bailly, C., Wilson, W. D., Eds.DNA and RNA Binders: From Small Molecules to Drugs; Wiley-VCH: Weinheim, Germany, 2003.
2. Sharma, S. K.; Morrissey, A. T.; Miller, G. G.; Gmeiner, W. H.; Lown, J. W. *Bioorg. Med. Chem. Lett.* **2001**, *11*, 769.
3. Baraldi, P. G.; Bovero, A.; Fruttarolo, F.; Preti, D.; Tabrizi, M. A.; Pavani, M. G.; Romagnoli, R. *Med. Res. Rev.* **2004**, *24*, 475.
4. Dervan, P. B. *Bioorg. Med. Chem.* **2001**, *9*, 2215.
5. Neidle, S. *Nat. Prod. Rep.* **2001**, *18*, 291.
6. Suckling, C. J. *Expert Opin. Ther. Patents* **2004**, *14*, 1693.
7. Shaikh, S. A.; Ahmed, S. R.; Jayaram, B. *Arch. Biochem. Biophys.* **2004**, *429*, 81.
8. Chaires, J. B.; Ren, J.; Hamelberg, D.; Kumar, A.; Pandya, V.; Boykin, D. W.; Wilson, W. D. *J. Med. Chem.* **2004**, *47*, 5729.
9. Fairley, T. A.; Tidwell, R. R.; Donkor, I.; Naiman, N. A.; Ohemeng, K. A.; Lombardy, R. J.; Bentley, J. A.; Cory, M. *J. Med. Chem.* **1993**, *36*, 1746.
10. Wilson, W. D.; Nguyen, B.; Tanious, F. A.; Mathis, A.; Hall, J. E.; Stephens, C. E.; Boykin, D. W. *Curr. Med. Chem.—Anti-Cancer Agents* **2005**, *5*, 389.
11. Wilson, W. D.; Tanious, F. A.; Mathis, A.; Tevis, D.; Hall, J. E.; Boykin, D. W. *Biochimie* **2008**, *90*, 999.
12. Soeiro, M. N. C.; De Souza, E. M.; Stephens, C. E.; Boykin, D. W. *Expert Opin. Invest. Drugs* **2005**, *14*, 957.
13. Athri, P.; Wenzler, T.; Ruiz, P.; Brun, R.; Boykin, D. W.; Tidwell, R.; Wilson, W. D. *Biorg. Med. Chem.* **2006**, *14*, 3144.
14. Lansiaux, A.; Dassonneville, L.; Facompre, M.; Kumar, A.; Stephens, C. E.; Bajić, M.; Tanious, F.; Wilson, W. D.; Boykin, D. W.; Bailly, C. *J. Med. Chem.* **2002**, *45*, 1994.
15. Neidle, S.; Kelland, L. R.; Trent, J. O.; Simpson, I. J.; Boykin, D. W.; Kumar, A.; Wilson, W. D. *Biorg. Med. Chem.* **1997**, *7*, 1403.
16. Vanden Eynde, J. J.; Mayence, A.; Johnson, M. T.; Huang, T. L.; Collins, M. S.; Rebholz, S.; Walzer, P. D.; Cushion, M. T.; Donkor, I. O. *Med. Chem. Res.* **2005**, *14*, 143.
17. Mayence, A.; Vanden Eynde, J. J.; Krogstad, F. M.; Krogstad, D. J.; Cushion, M. T.; Huang, T. L. *J. Med. Chem.* **2004**, *47*, 2700.
18. Bielawski, K.; Wolczynski, S.; Bielawska, A. *Pol. J. Pharmacol.* **2001**, *53*, 143.
19. Peixoto, P.; Liu, Y.; Depauw, S.; Hildebrand, M.-P.; Boykin, D. W.; Bailly, C.; Wilson, W. D.; David-Cordonnier, M.-H. *Nucleic Acids Res.* **2008**, *36*, 3341.
20. Hopkins, K. T.; Wilson, W. D.; Bender, B. C.; McCurdy, D. R.; Hall, J. E.; Tidwell, R. R.; Kumar, A.; Bajić, M.; Boykin, D. W. *J. Med. Chem.* **1998**, *41*, 3872.
21. Seaton, A.; Higgins, C.; Mann, J.; Baron, A.; Bailly, C.; Neidle, S.; van den Berg, H. *Eur. J. Cancer* **2003**, *39*, 2548.
22. Hranjec, M.; Piantanida, I.; Kralj, M.; Šuman, L.; Pavelić, K.; Karminski-Zamola, G. *J. Med. Chem.* **2008**, *51*, 4899.
23. Hranjec, M.; Kralj, M.; Piantanida, I.; Sedić, M.; Šuman, L.; Pavelić, K.; Karminski-Zamola, G. *J. Med. Chem.* **2007**, *50*, 5696.
24. Ismail, M. A.; Brun, R.; Wenzler, T.; Tanious, F. A.; Wilson, W. D.; Boykin, D. W. *Biorg. Med. Chem.* **2004**, *12*, 5405.
25. Del Poeta, M.; Schell, W. A.; Dykstra, C. C.; Jones, S.; Tidwell, R. R.; Czarny, A.; Bajic, M.; Bajic, Ma.; Kumar, A.; Boykin, D. W.; Perfect, J. R. *Antimicrob. Agents Chemother.* **1998**, *42*, 2495.

26. Mazur, S.; Tanious, F. A.; Ding, D.; Kumar, A.; Boykin, D. W.; Simpson, I. J.; Neidle, S.; Wilson, W. D. *J. Mol. Biol.* **2000**, *300*, 321.
27. Czarny, A.; Boykin, D. W.; Wood, A. A.; Nunn, C. M.; Neidle, S.; Zhao, M.; Wilson, W. D. *J. Am. Chem. Soc.* **1995**, *117*, 4716.
28. Kožul, M.; Stolić, I.; Žinić, B.; Bajić, M. *Croat. Chem. Acta* **2005**, *78*, 551.
29. Silber, A. M.; Colli, W.; Ulrich, H.; Alves, M. J.; Pereira, C. A. *Curr. Drug Targets Infect. Disord.* **2005**, *5*, 53.
30. Mohanakrishnan, A. K.; Hucke, A.; Lyon, M. A.; Lakshmikantham, M. V.; Cava, M. P. *Tetrahedron* **1999**, *55*, 11745.
31. Chadwick, D. J.; Chambers, J.; Meakins, G. D.; Snowden, R. L. *J. Chem. Soc., Perkin I* **1972**, 2079.
32. Agarwal, N.; Hung, C.-H.; Ravikanth, M. *Eur. J. Org. Chem.* **2003**, 3730.
33. Frigerio, M.; Santagostino, M.; Sputorre, S.; Palmisano, G. *J. Org. Chem.* **1995**, *60*, 7272.
34. Oszczapowicz, J.; Jaroszewska-Manaj, J.; Golimowska, K. *J. Chem. Soc., Perkin Trans. 2* **2000**, 2343.
35. McGhee, J. D.; von Hippel, P. H. *J. Mol. Biol.* **1976**, *103*, 679–684.
36. Rodger, A.; Norden, B. In *Circular Dichroism and Linear Dichroism*; Oxford University Press: New York, 1997.
37. Berova, N.; Nakanishi, K.; Woody, R. W. In *Circular dichroism Principles and Applications*, 2nd ed.; Wiley-VCH: New York, 2000.
38. Eriksson, M.; Nordén, B. *Methods Enzymol.* **2001**, *340*, 68.
39. Piantanida, I.; Palm, B. S.; Čudić, P.; Žinić, M.; Schneider, H.-J. *Tetrahedron* **2004**, *60*, 6225–6231.
40. Boger, D. L.; Fink, B. E.; Brunette, S. R.; Tse, W. C.; Hedrick, M. P. *J. Am. Chem. Soc.* **2001**, *123*, 5878.
41. Palm, B. S.; Piantanida, I.; Žinić, M.; Schneider, H. J. *J. Chem. Soc., Perkin Trans. 2* **2000**, 385–392.
42. Cantor, C. R.; Schimmel, P. R. In *Biophysical Chemistry*; WH Freeman: San Francisco, 1980; pp 1109–1181.
43. Mallena, S.; Lee, M. P. H.; Bailly, C.; Neidle, S.; Kumar, A.; Boykin, D. W.; Wilson, W. D. *J. Am. Chem. Soc.* **2004**, *126*, 13659.
44. Wang, L.; Carrasco, C.; Kumar, A.; Stephens, C. E.; Bailly, C.; Boykin, D. W.; Wilson, W. D. *Biochemistry* **2001**, *40*, 2511.
45. Munde, M.; Lee, M.; Neidle, S.; Arafa, R.; Boykin, D. W.; Liu, Y.; Bailly, C.; Wilson, W. D. *J. Am. Chem. Soc.* **2007**, *129*, 5688.
46. Miao, Y.; Lee, M. P. H.; Parkinson, G. N.; Batista-Parra, A.; Ismail, M. A.; Neidle, S.; Boykin, D. W.; Wilson, W. D. *Biochemistry* **2005**, *44*, 14701.
47. Spillane, C. B.; Fletcher, N. C.; Rountree, S. M.; vand en Berg, H.; Chanduloy, S.; Morgan, J. L.; Keene, F. R. *J. Biol. Inorg. Chem.* **2007**, *12*, 797.
48. Lansiaux, A.; Tanious, F.; Mishal, Z.; Dassonneville, L.; Kumar, A.; Stephens, C. E.; Hu, Q.; Wilson, W. D.; Boykin, D. W.; Bailly, C. *Cancer Res.* **2002**, *62*, 7219.
49. (a) Marczi, S.; Glavaš-Obrovac, Lj.; Karner, I. *Chemotherapy* **2005**, *51*, 217; (b) Marczi, S.; Glavaš-Obrovac, Lj.; Belovari, T.; Stojković, R.; Ivanković, S.; Šerić, V.; Piantanida, I.; Žinić, M. *Cancer Chemother. Pharmacol.* **2008**, *62*, 595.
50. Callegari, A. J.; Kelly, T. J. *Cell Cycle* **2007**, *6*, 660.
51. Yarden, R. I.; Pardo-Reoyo, S.; Sgagias, M.; Cowan, K. H.; Brody, L. C. *Nat. Genet.* **2002**, *30*, 285.
52. Rimkus, K.; Friederichs, J.; Rosenberg, R.; Holzmann, B.; Siewert, J.-R.; Klaus-Peter Janssen, K.-P. *Int. J. Cancer* **2006**, *12*, 207.
53. Dalton, B.; Nandan, M. O.; Moore, R. T.; Yangl, V. W. *Cancer Res.* **2007**, *67*, 11487.
54. Cunha-e-Silva, N.; Sant'Anna, C.; Pereira, M. G.; Porto-Carreiro, I.; Jeovanio, A. L.; de Souza, W. *Parasitol. Res.* **2006**, *99*, 325.
55. Mickisch, G.; Fajta, S.; Keilhauer, G.; Schlick, E.; Tschada, R.; Alken, P. *Urol. Res.* **1990**, *18*, 131.